INTERNATIONAL JOURNAL FOR NUMERICAL METHODS IN ENGINEERING
Int. J. Numer. Meth. Engng 2006; **68**:707–727
Published online 27 April 2006 in Wiley InterScience (www.interscience.wiley.com). DOI: 10.1002/nme.1720

Optimized damage detection of steel plates from noisy impact test

G. Rus[1,*,†], S. Y. Lee[1], S. Y. Chang[2] and S. C. Wooh[3]

[1]*Department of Structural Mechanics, University of Granada, Politécnico de Fuentenueva, 18071 Granada, Spain*
[2]*Department of Civil Engineering, University of Seoul, 90 Junneoung-Dong, Dongdaemoon-Gu, Seoul 130-743, Korea*
[3]*NDE Lab, Department of Civil and Environmental Engineering, Massachusetts Institute of Technology, Cambridge, MA 02139, U.S.A.*

SUMMARY

Model-based non-destructive evaluation proceeds measuring the response after an excitation on an accessible area of the structure. The basis for processing this information has been established in recent years as an iterative scheme that minimizes the discrepancy between this experimental measurement and sequence of measurement trials predicted by a numerical model. The unknown damage that minimizes this discrepancy by means of a cost functional is to be found. The damage location and size is quantified and sought by means of a well-conditioned parametrization. The design of the magnitude to measure, its filtering for reducing noise effects and calibration, as well as the design of the cost functional and parametrization, determines the robustness of the search to combat noise and other uncertainty factors. These are key open issues to improve the sensitivity and identifiability during the information processing. Among them, a filter for the cost functional is proposed in this study for maximal sensitivity to the damage detection of steel plate under the impact loading. This filter is designed by means of a wavelet decomposition together with a selection of the measuring points, and the optimization criterion is built on an estimate of the probability of detection, using genetic algorithms. Numerical examples show that the use of the optimal filter allows to find damage of a magnitude several times smaller. Copyright © 2006 John Wiley & Sons, Ltd.

KEY WORDS: inverse problem; quantitative non-destructive evaluation (QNDE); impact testing; genetic algorithms; wavelet analysis; noise filter

*Correspondence to: G. Rus, Department of Structural Mechanics, University of Granada, Politécnico de Fuentenueva, 18071 Granada, Spain.
†E-mail: grus@ugr.es

Contract/grant sponsor: Korea Research Foundation; contract/grant number: KRF-2005-M01-000-10230-0

Received 17 October 2005
Revised 9 February 2006
Accepted 17 February 2006

1. INTRODUCTION

Condition assessment technology and non-destructive evaluation (NDE) techniques have provided various solutions for safety of structures by means of detecting damage or defects from static or dynamic responses induced by external loading. A variety of techniques in this category have been developed in the last two decades. Based on analytical approaches, the existing studies [1–5] have limited capabilities in dealing with complex problems, primarily due to their limitations in handling different loading, boundary conditions and geometries in the analysis. Thus, many investigators developed a variety of numerical methods for assessing damage, e.g. damage index methods (DIM), inverse modal perturbation (IMP), and so on. These methods, despite their improvements over the conventional methods, still have some limitations, such as those associated with the divergence and instability problems in the numerical calculations, and the trap of minima, especially for large and complicated structures.

In recent years, direct search methods, such as neural networks, genetic algorithms (GA) and simulated annealing methods are developed and promisingly applied to the field of structural identification. Among them, GA attract our attention because of the fact that the technique requires significantly small amount of data in dealing with complex problems, while attaining global convergence as opposed to gradient-based methods. Suh *et al.* [6] presented a hybrid neuro-genetic technique that is able to identify the location and extent of damage in a beam or frame structure using only the frequency information. Mares and Surace [7] demonstrated the ability of the GA to identify damage in elastic structures. Friswell *et al.* [8] combined the genetic and eigensensitivity algorithms for locating damage. Chou and Ghaboussi [9] proposed a GA-based method to determine the location and extent of damage in truss structures from the measured static displacements. Krawczuk [10] presented a wave propagation approach to detect damage in beam structures based on GA and the gradient technique. On the other hand, Lee and Wooh [11] applied an advanced microgenetic algorithm for detecting damage of plate structures subjected to dynamic loading.

Despite the broad spectrum of applications for detecting damage, the numerical techniques may not be attractive from the practical point of view. The methods require a precise measurement of static or impact loading to the structure that needs to be input into the numerical model. Based on experimental work, precise control and measurement of input loading are extremely difficult because of errors arising from the physical structure. In particular, Kimoto and Hirose [12] found difficulties in correlating the numerical simulation of the surface-sensor system on the boundary of the experimental model, by modelling transducers as a distributed traction for the transmitter and using a weight function on the displacements for the receiver. In this approach, a transfer function is also inserted for the transducer–specimen system, as introduced by Schmerr [13]. These are also referred to as the *linear time-shift invariant* (LTI) and are used as Green functions to average within the transducer surface. The difficulty and disclaim in the sensor behaviour can be illustrated in their result these techniques, where they obtain discrepancies between the experimental and numerical signals of the order of 20% with respect to the maximum signal. They also introduced averaging of computations to enhance the results. Zhao *et al.* [14] also used the velocity instead of the displacement to model the receiver. Some efforts were made by Rus *et al.* [15] regarding which boundary conditions correctly simulate the effect of the transducer on the specimen model. The basis for these hypothesis and the linearity of the system are retrieved in the present numerical study.

The wavelet transform is a technique for the processing of signals of which the spectral countenance is non-stationary. It is defined in terms of a base function obtained by compression, dilatation and decay operations of the mother wavelet. In the wavelet transform, the signal spectrum is divided by an overlapping of pass band filters with constant relative bandwidth. Addison [16] gives an excellent overview of the potential that the novel wavelet analysis provides to different areas of science in the current days. Within the subject of mechanical systems, Kim and Kim [17] give a successful wavelet ridge analysis of the correlation of reflected to incident wave magnitude ratio over the time and frequency to correlate an experiment with a bending beam model. This application is merged with numerical methods by Li *et al.* [18] who use the wavelet finite element method (WFEM) in modal analysis to find cracks with the aim of solving accurately the crack singularities. On the other hand, wavelets can also be used for noise removal, which is our objective in this study. Messina [19] compares wavelets for noise removal against differentiator filters, concluding that they provide very similar performance, which is expectable due to some common mathematical basis. In a similar approach, Yang *et al.* [20] apply envelope complex wavelet analysis correlation to efficiently discriminate noise from the signals in an experimental case. On the other hand, a standard wavelet analysis is used in this study as one of the two filtering tools within a novel framework of optimization of the search methodology.

Being critical for the practice of NDE, the issue of the probability of detection (POD) has only been addressed independently, under the name of identifiability, in statistics and mathematics, with a wide application in chemistry and physics. However, in the field of non-destructive testing, only observational comments have been made. Only Liu and Chen [21] discussed as identifiability the relationship between the number of measurements and the number of degrees of freedom to establish a necessity condition. Tarantola and Valette [22] examine the inversion theory under a probabilistic formulation and introduce probability density functions in the model and the *a priori* information about the parameters to explain the robustness of the inversion and to obtain a non-single-valued output for the parameters. In this study, an estimate of the POD is designed from the minimization search approach as a criteria to be optimized for the design of the formulation.

The forward and inverse procedures are presented for the identification of damage in steel plates by combining the FEM as the numerical procedure for the simulation of the effect of the defect on the response to impact loading, and a parametrization of the defect in combination with a calibrating cost functional with an optimized noise filter and GA for the optimization and search procedures. More realistic simulated noise is added in the numerical simulation of the experiment by introducing a Gaussian force at the excitation pulse along the time, which exhibits qualitative differences to noise added directly to the computed measurements. However, without an efficient searching scheme, it is very difficult to solve this kind of inverse problems. In this study, we propose an efficient method to identify damage in structures by combining GA with a filter for noisy dynamic response. This filter weights the wavelet coefficients, time windows and measurement points. Then, the POD is approximated from certain simulated values of the measurements. Finally, the proposed method determines the best measuring points, wavelets levels and time windows for locating and evaluating damage on steel plates using the optimized filter and cost functional.

2. FORWARD PROCEDURE

2.1. Damage model

In order to measure the dynamic data from damaged plate structure, the FEM is implemented to simulate the forward procedure. In a finite element formulation for solving a forward problem, the stiffness matrix of a structural system is expressed in terms of its material properties, geometry, and boundary conditions. In this paper, the damage is defined as the stiffness reduction factor $\beta^{(m)}$ at one or more local areas [7, 11, 23].

The structure is discretized into a set of finite elements categorized into undamaged and damaged states of different degradation levels. For such a model, the global stiffness matrix of the mth damaged element can be expressed as

$$\tilde{\mathbf{D}}^{(m)} = \beta^{(m)}\mathbf{D}^{(m)} \tag{1}$$

where $\mathbf{D}^{(m)}$ is the stiffness in its original (undamaged) state. Note that the tilde symbol above a variable is used to denote the damaged state. The stiffness matrix of the damaged element in the local coordinates can now be written as the volume integral of the form

$$\tilde{\mathbf{K}}^{(m)} = \beta^{(m)} \int_V \mathbf{B}^{(e)\mathrm{T}}\tilde{\mathbf{D}}^{(m)}\mathbf{B}^{(e)}\,\mathrm{d}\Omega \tag{2}$$

where $\mathbf{B}^{(e)}$ is the strain–displacement matrix of the element e, and the superscript T denotes the transpose operator. Note that $\mathbf{B}^{(e)}$ is a property that is independent of damage, thus it is applicable to all the elements e, whether damaged or undamaged.

The governing equation of motion of the system is written in the form

$$\mathbf{M}\ddot{\mathbf{u}} + \mathbf{K}\mathbf{u} = \mathbf{r} \tag{3}$$

where $\mathbf{u}$ and $\ddot{\mathbf{u}}$ are the displacement and acceleration vectors, $\mathbf{M}$ and $\mathbf{K}$ are the mass and stiffness matrices and $\mathbf{r}$ is the time history of the applied load, respectively. To advance the solution of this equation in time, we use Newmark's direct integration method [24], in which the time dimension is represented by a set of discrete points with equal time increment of Δt. The following naming convention is adopted: the value of a function $\xi(t)$ at time $t = n\Delta t$ is denoted by the index n as

$$\xi(t) = \xi(n\Delta t) = \xi[n], \quad n = 0, \ldots, N \tag{4}$$

where $N + 1$ is the total number of temporal discretization points for the entire duration of time T_d.

2.2. Noise effect

In order to consider unexpected errors in the measured displacements or accelerations, the usual option is to introduce the effects of random noise by adding Gaussian noise directly to the values computed by the FEM. An alternative approach is proposed here for simulating the incomplete signal from the structure with the noise effects, which consists of an external random force excitation applied over the complete time period, and normal to the plate over the inboard area. This simulates the error arising from the uncertainty of the interaction between the impactor or transmitter, as well as the ambient noise and other coherent noise sources.

From the practical point of view, the latter aims to study a situation closer to the real structure, providing qualitative similarities to the error induced in the physical system.

If the noise effects are considered directly at the measured response on the kth node, a Gaussian (normal) random number generator is used to generate a series of random numbers $\zeta_k[n]$ with standard deviation $\sigma = 1$ and zero mean. This series simulates a random process $\zeta(t)$, and the simulated measurements are given by

$$\Phi^x(p;\sigma_n)[n] \simeq \Phi(p)[n] + \mathrm{RMS}(\Phi)\zeta[n] \tag{5}$$

If ambient noise is simulated, the random noise tractions t^n are made of a random process ζ with random distribution of zero mean and standard deviation $\sigma = 1$, and defined from a spectrum $h^t(t)$ (in the time domain, or conversely $H^t(\omega)$ in the frequency domain) of the noise and the root mean square of the applied tractions t ($*$ stands for convolution product, in the time domain),

$$t^n[n] = \mathrm{RMS}(t)h^t[n] * \zeta[n] \tag{6}$$

where RMS stands for the root mean square. This noise on the force can be estimated to affect the measurements Φ^x through a spectrum h^Φ that depends on the transfer function of the specimen and the input noise spectrum,

$$\Phi^x(p;\sigma_n)[n] \simeq \Phi(p)[n] + \mathrm{RMS}(\Phi)h^\Phi[n] * \zeta[n] \tag{7}$$

In the following numerical experiments, only white noise (uniform frequency spectrum $H(\omega_j)$) will be used, but in case the process is assigned a non-uniform frequency spectrum, that can be estimated during the calibration process, the following relationship can be extracted:

$$\sigma_n = \sqrt{\frac{1}{N^2}\sum_{j=0}^{N-1}|H_j|^2} \tag{8}$$

Redundant measurements are an effective way to reduce the effect of noise. If the noise is assumed Gaussian with zero mean and standard deviation σ_n, an effective way to reduce it is increasing the number of measurements N. Then, since the system is linear we can just take it into account substituting the measurements with their mean values, and the noise will reduce with a factor $1/\sqrt{N}$,

$$\tilde{\Phi} = \frac{1}{N}\sum_k \Phi_k \quad \Rightarrow \quad \frac{1}{N}\sum_k (\Phi_k + H * \zeta_k) = \tilde{\Phi} + \frac{H}{N} * \sum_k n_k = \tilde{\Phi} + \frac{H}{\sqrt{N}} * \zeta \tag{9}$$

3. INVERSE PROCEDURE

The inverse procedure presented aims at characterizing damage in a structure and determine its extent (degree of degradation) and location. The procedure consists of two testing steps: (1) to disturb a structure with a known excitation function (usually an impact loading described by a delta function) and (2) to measure its response (transient time history or a waveform representing the displacements, usually obtained by accelerometers) at one or more locations in the structure. We assume that the dynamic behaviour of the structure in its intact and damaged

states is predictable using a well-calibrated model. Then, the measured signal is processed to solve the *inverse problem*, i.e. to determine the changes in the structure from its original state. Since the entire inverse procedure is associated with forward problem solutions in each iteration step, the rate of convergence depends on the complexity level of the forward formulation.

A GA search tool [11, 25] is used to minimize the discrepancy between the experimental readings and the numerically predicted trial response, by means of a cost functional designed to calibrate for coherent uncertainties and noise, and providing maximal robustness and sensitivity. Thus, we focus on determining best cost functional for detecting damage from responses with noise. Moreover, we propose and optimal choice of measuring points as well as time windows and wavelet level filters for better sensitivity to noise effects. The criterion for this is chosen in a rational way so as to maximize the POD.

3.1. Cost functional

The inverse problem of the defect search is carried out with an iterative strategy based on the minimization of some discrepancy. The discrepancy is a vector of values or a function that can be discretized (represented by a vector). Since two vectors cannot be compared directly, a scalar number (called cost functional) is derived from them, in order to be able to minimize that discrepancy. The goal of this work is to design that cost functional as well as the discrepancy in such a way that its minimization can be carried out for the smallest possible defect and including the largest possible magnitude of noise.

The readings from the sensors do not need to coincide with the measurements to analyse, which are vectors that will be denoted by ψ for the theoretical or synthetic case, and ψ^x for the experimental case. For a good solution, several conditions can be desirable for the measurements. Unlike the readings, the measurements should be calibrated magnitudes, so that they gain independency from the ambient conditions during the experiment. They should also be a dimensional, so as not to prejudice the numerical conditioning of the search algorithms. A measurement $\overset{\circ}{\psi}$ in the undamaged state of the specimen is defined in order to calibrate the acquired information for some coherent noise and amplitudes. The measurement to analyse is therefore defined from Equation (10) or (13) as

$$\Phi = \frac{\psi - \overset{\circ}{\psi}}{\mathrm{RMS}(\overset{\circ}{\psi})} \tag{10}$$

where the RMS values are defined for a discrete function f in time domain $f(t_i)$ or frequency domain $F(\omega_j)$ at N sampling points as

$$\mathrm{RMS}(f) = \sqrt{\frac{1}{N}\sum_{i=0}^{N-1} f(t_i)^2} = \sqrt{\frac{1}{N^2}\sum_{j=0}^{N-1} |F(\omega_j)|^2} \tag{11}$$

A *residual* γ is defined from the misfit or *discrepancy* $\Phi^x - \Phi$ between the measurements. A *filter* w is included, which will be later defined for optimizing the residual,

$$\gamma = w(\Phi^x - \Phi) \tag{12}$$

There are many options for designing a cost functional. The necessary conditions are that a full coincidence of prediction and measurement (zero discrepancy) should coincide with the

absolute minimum of the cost functional, and that of uniqueness of this minimum. The L-2 norm, in a standard metric Euclidean space of these residual vectors, is usually a good choice of cost functionals, since it fulfils naturally the former conditions and is numerically smooth and well conditioned. This quadratic or least-squares-type definition is meaningful in a probabilistic sense, as well as in an algebraic sense as a measure of a distance between bad and good results. The *cost functional* f or fitness function is chosen after a residual vector γ of size N_i as

$$f = \frac{1}{2}|\gamma|^2 = \frac{1}{2}\frac{1}{N_i}\sum_{i=1}^{N_i}\gamma_i^2 \tag{13}$$

It is useful to define an alternative version of the cost functional denoted as f^l, with the property of improving the sensitivity while approaching the optimum, just by introducing a logarithm and a small value ε to ensure its existence. This definition particularly enhances the convergence speed when the minimization is tackled by with GA or other random search algorithms (see Reference [26]),

$$f^l = \log(f + \varepsilon) \tag{14}$$

The parametrization can be defined within the subject of inverse problems as a description or characterization of the sought information (i.e. damage characterization) with a reduced set of variables. The issue of parametrization is complicated due to the relationship with many considerations of the inverse problem. Many inverse problems are ill-posed: solutions may not exist, they could be unstable and non-converging, or there may exist multiple solutions. This is true especially when we are dealing with a large number of parameters. From the conceptual point of view, it can be seen as the most powerful means of regularization of inverse problems, since it provides *a priori* information in the form of strong hypothesis in the possible forms of the sought defects. The choice of parameters has crucial implications in the convergence, the sensitivity of the result and the decoupling of their dependence to the measurements.

To follow these considerations, a reduced set of parameters is designed by allowing a reduced set of individual damages (allowing multiple defects, but limiting the number), each of them described in a simplified way by their position and extent. The two coordinates for the position are decoupled by using the x and y position of the damaged area and its extent $1-\beta$, where β is the stiffness reduction factor. The parameters are denoted by a vector p of length N_p. The parameter that best describes the real defect is denoted by $\tilde{p}$,

$$p = \{x_1, y_1, 1-\beta_1, x_2, y_2, 1-\beta_2, \ldots\} \tag{15}$$

At this point, the inverse problem of defect evaluation can be stated as a minimization problem, that can be constrained, as finding p such that,

$$\min_p f(p) \quad \text{or} \quad \min_p f^l(p) \tag{16}$$

3.2. Probability of detection

Three variables will be considered in the problem of maximizing the POD, the level of noise, denoted by σ_n (regardless of whether it is simulated on the forces, measurements, or any other way), the size of the defects, denoted by p and the cost functional that collects the effects of those in a scalar $f(p, \sigma_n)$, through the definitions above.

In this procedure, we start assuming the case of only one possible position for the defect. Two cost functionals for two independent cases is defined. First, if a damaged specimen with a infinitesimal defect $\tilde{p} = p$ is tested, and it is assumed that the measurements contain no noise ($\sigma_n = 0$), and two cost functionals $f(p, \sigma_n)$ are evaluated, one for the correct parameter $\tilde{p}$ and another without defect $p = 0$, a measure for the rate of variation of the range of values of f with respect to some magnitude of the defect can be defined as $f_{,p}$,

$$f_{,p} = \frac{\mathrm{d}^2 f}{\mathrm{d}p^2} = \lim_{p \to 0} 2 \frac{f(p, 0) - f(0, 0)}{p^2} \tag{17}$$

For a larger defect p, that cost functional without noise effects will be called f^d, and can be approximated by the former, taking into account that $f(0, 0) = 0$,

$$f^p = f(p, 0) = 0 + \tfrac{1}{2} f_{,p} p^2 + \text{hot} \tag{18}$$

The reason that the first derivative is not considered is the quadratic nature of the cost functional. Second, if a undamaged specimen ($\tilde{p} = 0$) is tested with noise σ_n, the evaluation of one each functionals with and without noise provide an approximation for its rate of variation with the amount of noise, $f_{,n}$, in a similar formulation,

$$f_{,n} = \frac{\mathrm{d}^2 f}{\mathrm{d}n^2} = \lim_{\sigma_n \to 0} 2 \frac{f(0, \sigma_n) - f(0, 0)}{\sigma_n^2}, \quad f^n = f(0, \sigma_n) = 0 + \tfrac{1}{2} f_{,n} \sigma_n^2 + \text{hot} \tag{19}$$

The ratio between those derivatives gives the linearized (first order) approximation of the relationship between the amount of noise and the size of the defect, which is a function of the position of the defect, and the ratio p/σ_n becomes independent of the form of the cost function f,

$$\frac{f^p}{f^n} \simeq \frac{f_{,p}}{f_{,n}} \left(\frac{p}{\sigma_n} \right)^2 \tag{20}$$

The POD is now defined as the probability that the alteration of the cost functional by the defect is bigger than the effect of the noise on that cost functional, $\text{POD} = P(f^n \leqslant f^p)$. If the noise is assumed to be a stochastic process with a normal distribution, since f is a sum of $N_m N_t$ squares of normal processes (N_m is the number of measurements and N_t is the number of timesteps when time is discretized), it holds a $f^n \to \alpha \chi^2$ distribution with the number of degrees of freedom $D = N_m N_t$ and α a multiplicative constant. The χ^2 distribution can be approximated, if $D > 10$, by a gaussian distribution $N(\mu, \sigma)$ with mean $\mu = D - 2/3$ and $\sigma = \sqrt{2D}$.

If f^n is evaluated a single time, it will tend to give the mean value μ' of its random process $f^n \to \alpha N(\mu, \sigma) = N(\tilde{\mu}, \tilde{\sigma})$. This allows to approximate the value of α, and hence,

$$\alpha = \frac{f^n}{D - 2/3} \quad \Rightarrow \quad \tilde{\mu} = \alpha \mu = f^n, \quad \tilde{\sigma} = \alpha \sigma = f^n \frac{\sqrt{2D}}{D - 2/3} \tag{21}$$

Provided that the probability is $P(z \leqslant x) = \alpha = F(x)$ and $F(x) = \int_{-\infty}^{x} f(y)\, \mathrm{d}y$ is the normal cumulative distribution function with zero mean and standard deviation $\sigma = 1$, whose inverse is

$x = G(\alpha) = G(F(x))$, the POD is,

$$\mathrm{POD} = P(f^n \leqslant f^p) = F\left[\frac{f^p - \tilde{\mu}}{\tilde{\sigma}}\right] \simeq F\left[\frac{D - 2/3}{\sqrt{2D}}\left(\frac{f_{,p}}{f_{,n}}\left(\frac{p}{\sigma_n}\right)^2 - 1\right)\right] \tag{22}$$

$$\frac{p}{\sigma_n} \simeq \sqrt{\frac{f_{,n}}{f_{,p}}\left(1 + G[\mathrm{POD}]\frac{\sqrt{2D}}{D - 2/3}\right)} \tag{23}$$

The maximization of the POD is therefore equivalent to the minimization of p/σ_n, and in the case of several possible defect positions, a *minimax* criterion (pessimistic) is introduced to ensure that no defects are left undetected,

$$\max \mathrm{POD} \quad \Leftrightarrow \quad \min\left(\max_{\text{position}} \frac{p}{\sigma_n}\right) \tag{24}$$

A similar conclusion to that obtained in Equation (9) can be drawn for the ratio $f_{,n}/f_{,p}$ when the number of measurements is multiplied by a factor N, which can be proved to reduce by a factor $1/\sqrt{N}$.

3.3. Optimization of filters

In this study, the optimization of the filters for reducing noise effect is carried out with the criterion of maximizing the POD.

The weight filter w is a user-selectable filter. The filter can be defined for giving more weight on certain important frequencies, time windows or measuring points, while reducing or eliminating the others. The benefit of this is that certain selections provide more sensitivity to the defect and less sensitivity to the noise, while others provide the opposite, which would damage the overall quality of the information available from the readings.

A discrete wavelet decomposition is introduced in order to separate the detail levels in the signal and the time dimension. If the wavelet transform of a function $\mathrm{WT}(f)$ provides a set of detail coefficients $c(t_i, l)$, $i = 1, \ldots, N_t$, $l = 1, \ldots, N_l$, that allow to recover the original signal by their inverse transform $f(t_i) = \mathrm{IWT}(c(t_i, l))$ together with some approximation coefficients. A `rbio6.8` wavelet is used throughout, since it empirically seems to provide a better sensitivity. The reason is probably the high time-resolution that it provides, as well as a mother wave with a shape compatible to that of the recorded signal. The detail coefficients can be used for defining the weighting filter $w = \{w_m, w_i, w_l\}$ by the composition of three filters w_m to select the measurement, w_i to select the time window (that is defined for few points and then oversampled), and w_l to select the detail level, as

$$w(f_m(t_i)) = \mathrm{IWT}(w_m w_i w_l c_m(t_i, l)) \tag{25}$$

Figure 1 illustrates a flow chart for optimal filter w computed by the finite element analysis and GA applied in this study. Using w computed by optimization of the filter. The location and extent of damage is finally determined by running GA at a second stage, as shown in Figure 2.

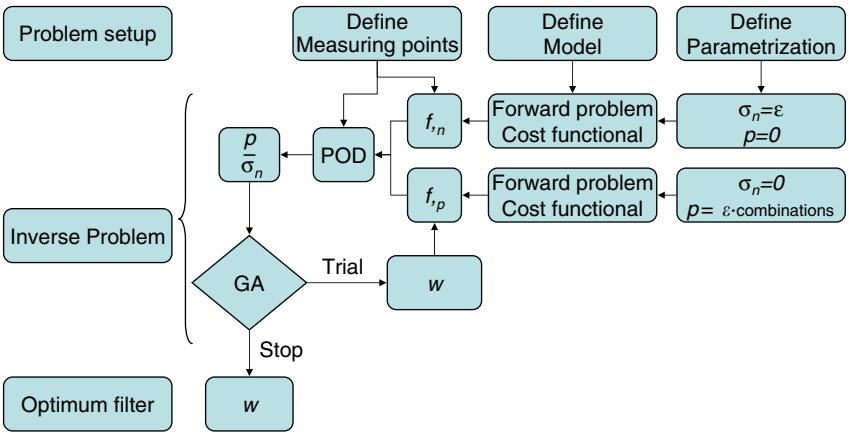

Figure 1. A flow chart for determining optimal filter w^f/w^Φ using the GA.

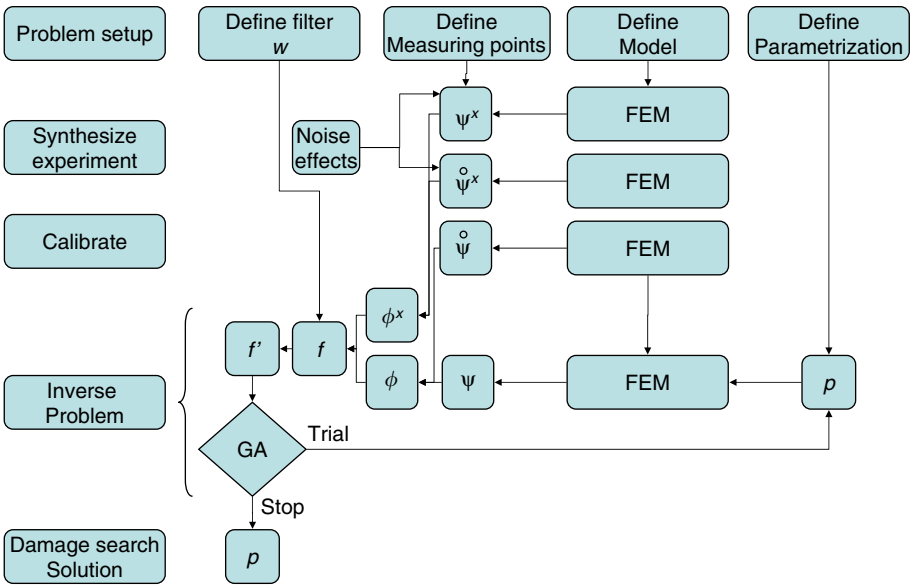

Figure 2. A flow chart for determining location and extent of damage using w^f/w^Φ.

4. NUMERICAL EXAMPLES

4.1. Numerical model

A steel plate of dimensions 1×1 m and thickness 1 cm is tested. The boundary conditions are clamped on two opposed sides as shown in Figure 3. An impact force is applied at the marked

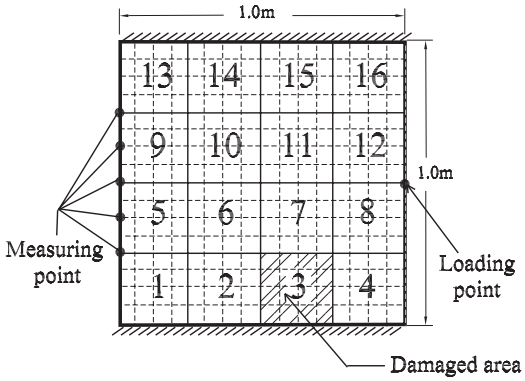

Figure 3. Numerical model of the steel plate.

point, and measurements are made at the 15 points distributed over a regular 3×5 mesh. The impact load has a magnitude of 10 MPa and a duration of 2 ms, whereas the measurement recording period is 100 ms.

Some assumptions are made for the simulation of the impactor and the receiver. The signals generated by the impactor are described by prescribing the pressure boundary conditions $q_i(x, t)$. The validity of this assumption was studied by Rus *et al.* [15] by comparing the results between the two extreme cases of Neumann and Dirichlet boundary conditions. This stress is assumed to be distributed uniformly over the area of contact. Thus, the impact pressure can be prescribed by multiplying the constant pressure q_i and its phase or time delay $\varphi(t)$,

$$q_i(x, t) = q_i \varphi(t) \tag{26}$$

The output signal from the receiver is assumed to be the time average of displacements (or accelerations) of the points on Γ_n, the area of contact between the specimen and the receiving transducer. Shear stresses cannot be sustained on the specimen–impactor or the specimen–receiver boundaries, which means that only normal components are taken.

$$u_i(t) = \int_{\Gamma_n} u_i(\Gamma, t)\, \mathrm{d}\Gamma \tag{27}$$

In order to determine optimal mesh size and time step for GA, the estimated errors are computed for different finite element mesh refinements and time steps as shown in Figure 4. It can be observed that the combination of a time step of 0.4 ms and a mesh discretization in 16×16 elements gives an error sufficiently below 5%.

Figure 5 shows the deformed shapes for different time steps of plates with undamaged and damaged areas. From the figure we can observe the different deformed shapes between two plates with undamaged and damaged areas. Notice the time delays by comparing with the waveforms shown in Figure 6. This represents the time required for the shock wave to travel the distance between the loading and measuring points. It can be also observed that the wave of plate without damaged area arrives at an earlier time, and the difference becomes more dramatic as time increases. This is predictable because the stiffness of undamaged plate in the axial direction is higher than that of damaged plate, and consequently the wave propagation

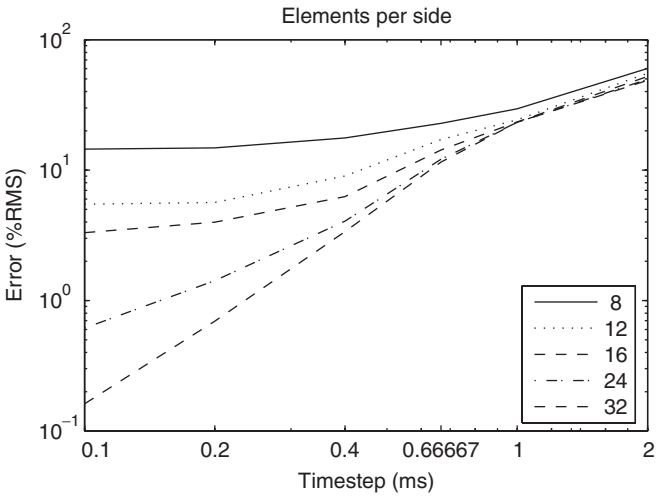

Figure 4. Evolution of estimated relative error (%) for different time steps and divided mesh numbers of plate.

speed increases in that direction. An increased wavespeed results in shorter arrival times and smaller wavelengths.

A sample of the corresponding signal samples for each of the two noise models is presented in Figure 7. It can be noted that the nature of the noisy signal is very different, since the specimen subject to boundary condition force noise acts as a low pass filter, eliminating the high frequency components, but the noisy data is in average more deviated from the original, as occurs in real experiments. This effect cannot be removed easily by filtering the signal, but requires of the proposed calibration scheme as well as of the cost functional minimization strategy to be overcome.

4.2. Optimal damage detection

4.2.1. Optimal filtering. As mentioned earlier, the proposed filter for reducing the noise effect and improving the sensitivity is composed by three superposed filters: one for the time window, which is defined by cubic interpolation from five points with values 1 or 0; another for five levels of the `rbio6.8` wavelet decomposition, also with 1/0 values; and another for selecting a fixed number of measurement points out of the 15 possible ones described in the geometry. Figure 8 shows several examples of the effect of selecting different combinations of measurement points on the ratio p/σ_n, which gives a relative measure of the size of the defect that can be detected, and therefore an indication of the POD. An example of the wavelet decomposition is given in Figure 9.

Now, a standard GA is implemented for the search of the defect and the optimal filter. This is done first by considering only the wavelet-level selection and time windowing, then by considering only the selection of the measurement, and finally by considering all together. In GA, both real coded and bitstring coding algorithms have been used, leading the latter to better results. The characteristic parameters are a crossover fraction of 0.6 and a migration fraction

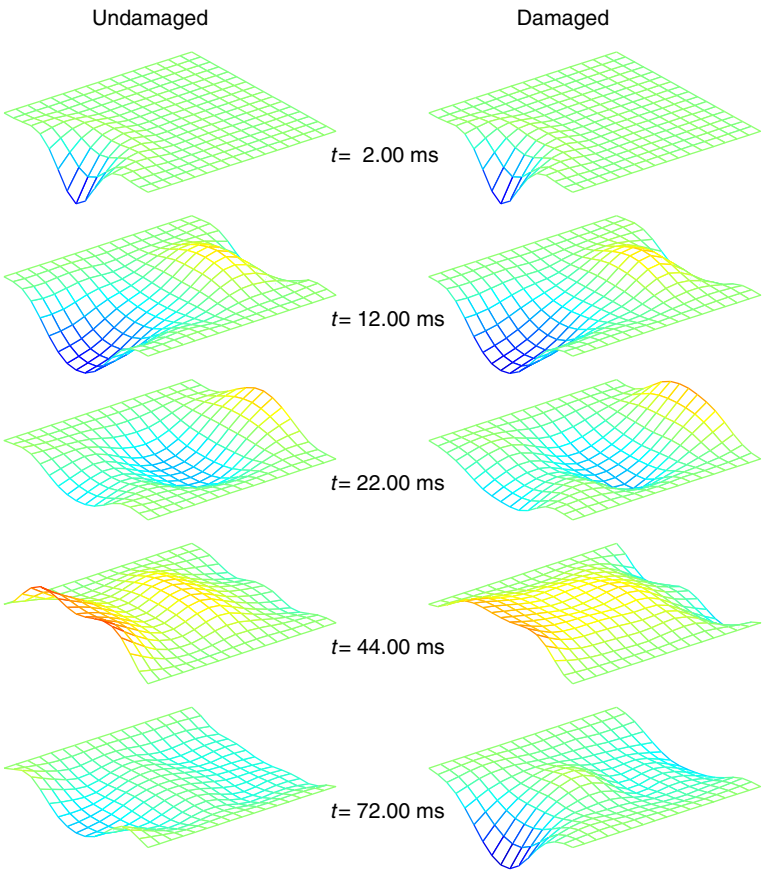

Figure 5. Deformed shapes at different time steps of plates with undamaged and damaged areas.

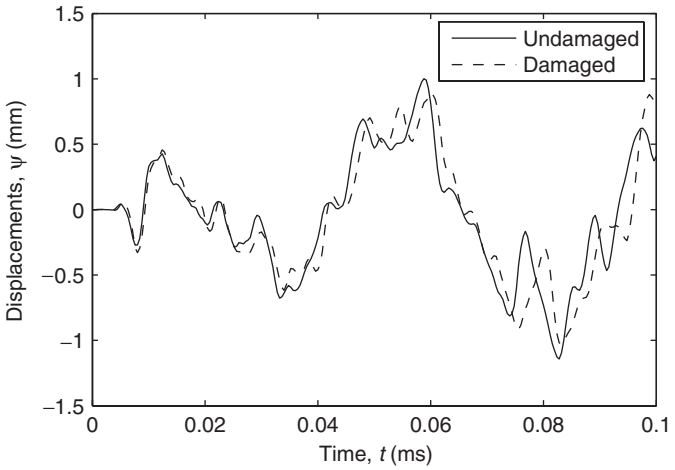

Figure 6. Dynamic displacements of two steel plates with undamaged and damaged areas.

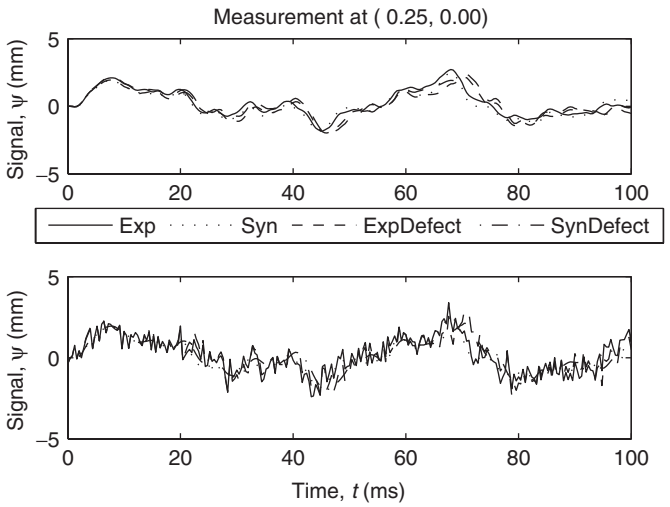

Figure 7. Sample signals for each noise model. Signal with and without noise for undamaged and damaged specimen. (Above) Noise as boundary condition force. (Below) Noise as recorded displacement perturbation.

of 0.4. The number of generations is 100, and the number of individuals in the population is 30. For the optimization of the POD, the term f_d/f_n is approximated by finite differences using $\varepsilon_n = 0.0001$ and $\varepsilon_p = 0.02$.

The wavelet level and time window optimization is performed in Figure 10. Binary coding is used in this case, where 5 bits are used for the five wavelet levels, and 5 bits for the five reference points in time. The results show that the last 40% of the time tends to be removed in all cases, since it provides more noise. In some cases the window around 20 ms is also removed. Wavelet level 5 is always removed, also because it concentrates most of the noise effect, and is less sensitive to the position of the defect, and sometimes also levels 2 and 4.

Figure 11 shows a similar optimization for selecting the optimum position of the measurement points. A binary coding is also used, with the minimum necessary number of bits to count all the possible combinations of sensor collocations. Figure 12 combines the two former optimizations simultaneously, giving a slightly different result that in the independent case. A binary coding is used with the sum of the former number of bits. Some minor variations are observed in the wavelet and time window, but bigger changes are found in the measurements selection, especially when more measurements are considered. This reflects that there are several combinations of sensor collocations that provide a similar improvement of the POD.

It is interesting to note that from all the examples shown so far, there do not seem to be simple rules for the optimum collocation of sensors, but the improvement in the damage that can be detected is important. This suggests that a numerical optimization of the sensor collocation, using the principles proposed here, pays back.

4.2.2. Final damage search. Figure 13 studies the effect of the number of measurements as well as the effect of the optimization of the weight filter on the search of single defect. The

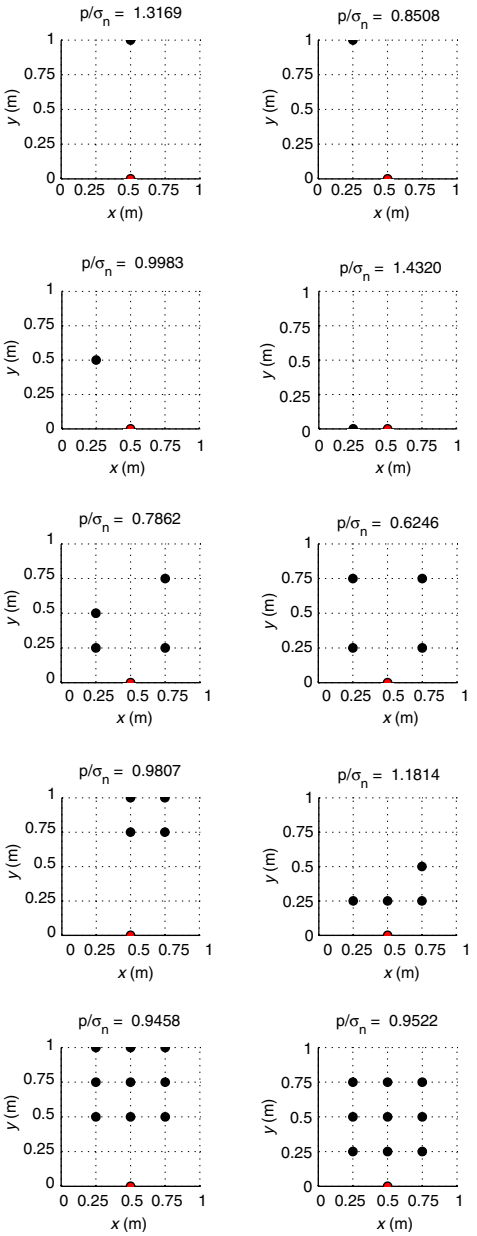

Figure 8. Variation of p/σ_n (indicating the POD) with the selection of measuring points (black dots) on the geometry of the plate. (Above) Case of 1 measurement. (Middle) Case of 4 measurements. (Below) Case of 8 measurements.

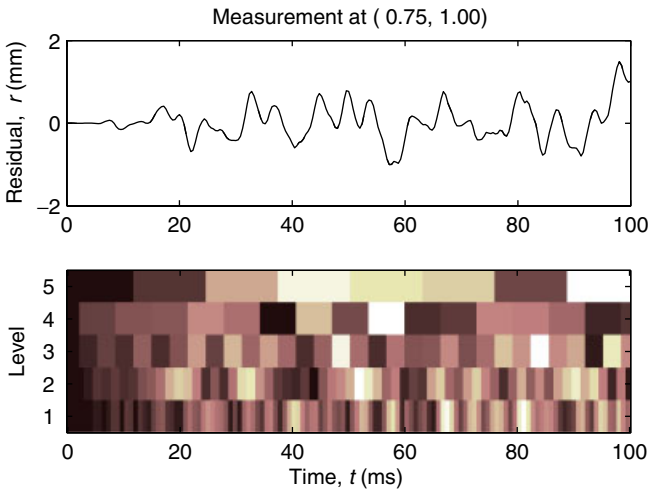

Figure 9. Residual for a single measurement and its wavelet decomposition into coefficients at several levels.

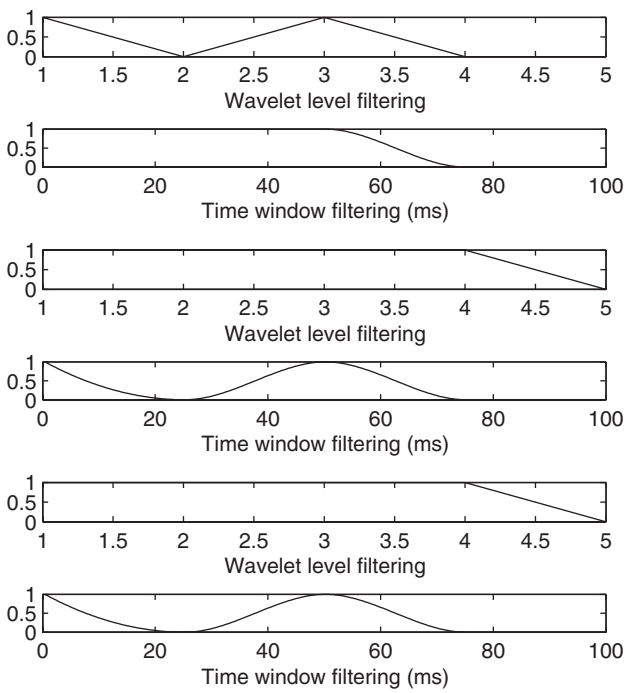

Figure 10. Best wavelet and time window weight filter for the cases of 1 measurement (above), 2 (middle) and 4 (below).

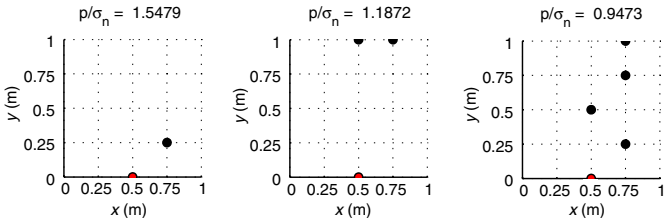

Figure 11. Best measurement positions for the cases of 1, 2 and 4 measurements, respectively.

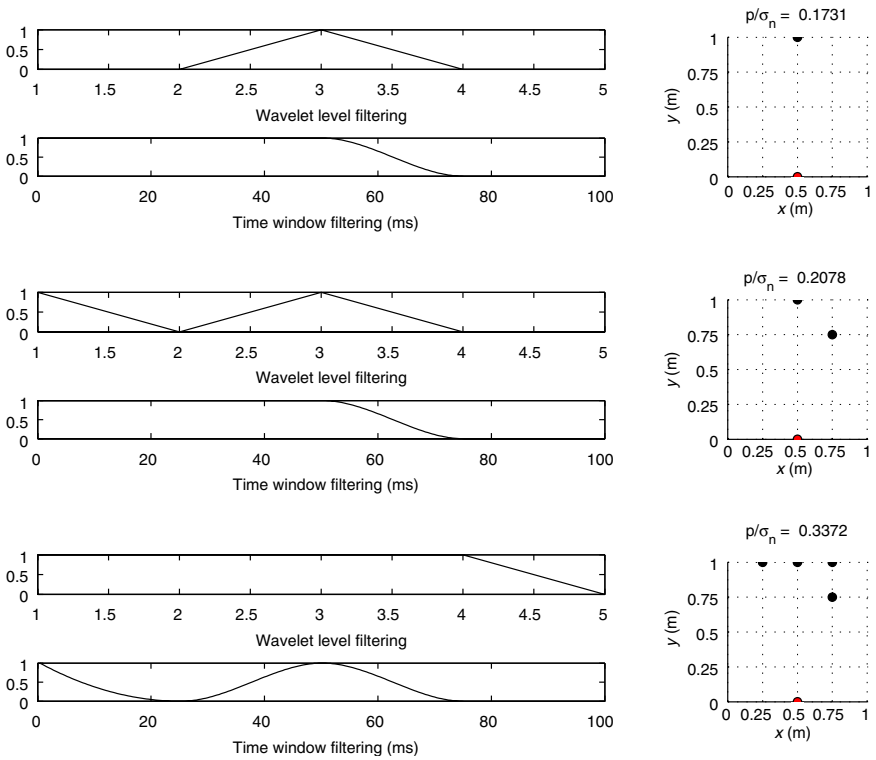

Figure 12. Best combined weight filters for the cases of 1, 2 and 4 measurements, respectively.

figure represents a map with the value of the cost functional when a trial defect is tested on each of the 4×4 possible damaged areas, using the correct value of it. A noise of $\sigma_n = 0.5$ (50%) and of force type is included in all cases. In the search procedure, a binary coding has been also adopted, with a gene defined with 10 bits for one defects and 20 for two, in which 2 bits define the horizontal position, 2 bits the vertical, and 6 bits the damage factor, which allows a range of 64 different values. The use of the optimum filter improves the contrast between the cost functional on the correct and incorrect trial points, which is indirectly a

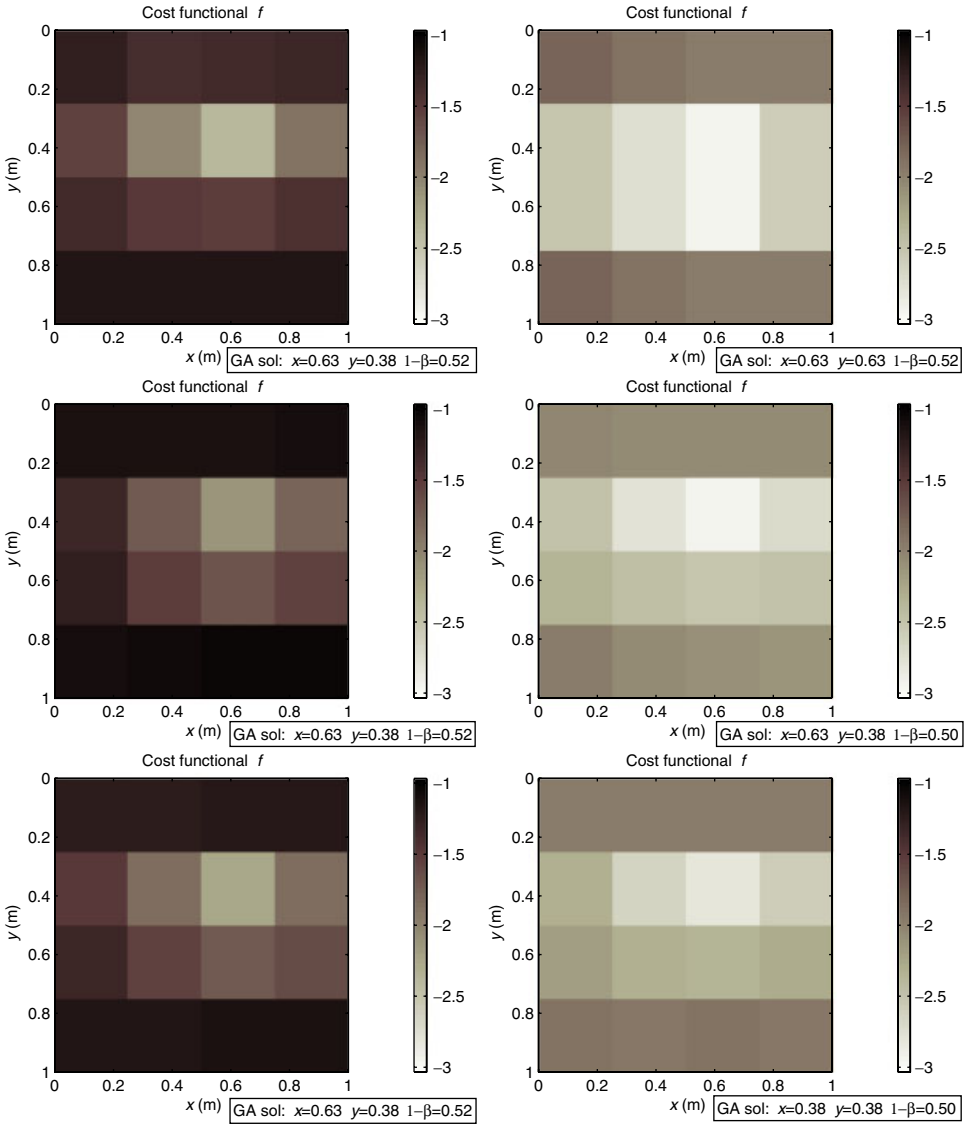

Figure 13. Searching of single damage. (Left) Without weight filter. (Right) With optimum filter. (Above) Case of 1 measurement. (Middle) Case of 2 measurements. (Below) Case of 4 measurements.

reason for improving the POD. It is observed that the overall value of the cost functional also decreases and is smoother, which also contributes to the numerical convergence of the search, and reduces the risk for falling in false local minima. Figure 14 shows the evolution of the fitness of the search as the generations progress.

Finally, in the case of optimal filtering, the GA fully recover the location and extent of the defect despite the noise of 50%, whereas without filter, it is found with a relative error of 3%.

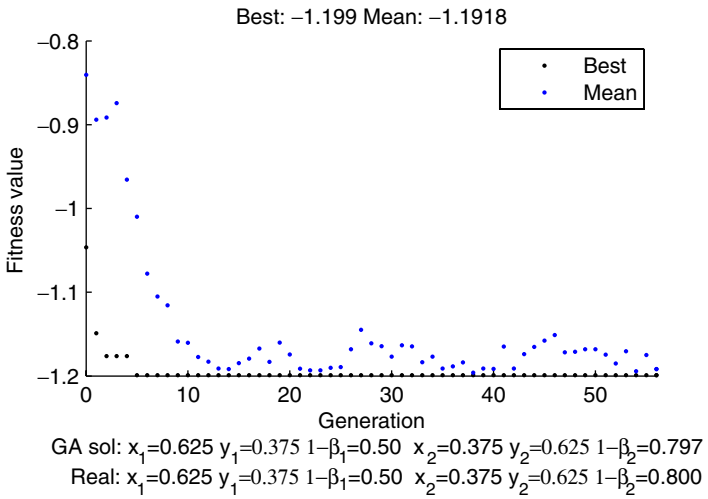

Figure 14. Searching of two damages as the increased generations.

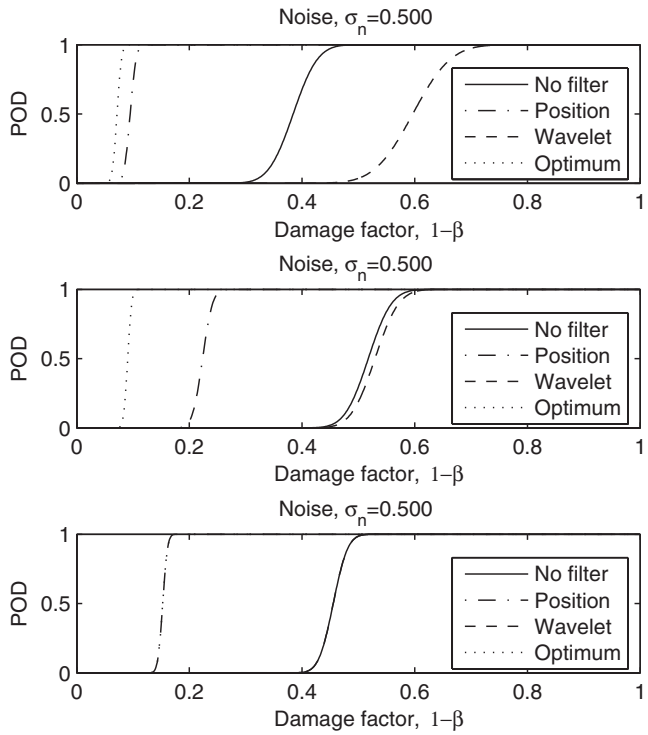

Figure 15. POD without filtering and with filtering. Case of 1, 2 and 4 measurements, respectively.

4.3. POD for different filters

The POD is estimated from a simulation of the noisy signal to estimate the mean noise effect f_n and the effect of all the 4×4 possible defects f_p processed from Equation (22). The results are shown in Figure 15 for the case of no weight filter, wavelet filter, position filter and optimum filter to show the improvement. An increase factor between 3 and 5 is observed in the size of the minimum damage that can be detected if the optimum filter is applied. This improvement is even significant if a partial filter is applied.

5. CONCLUSION

This paper presents an effort to integrate all the information recorded in the measurements from impact testing in a generalized inversion scheme. The goal of this study is to avoid overlooking rich data that may be crucial to combat the noise that hide difficult defects. The key principles of the search algorithm are, first, an advanced FEM model to predict the dynamic behaviour of plate under the impact loading; second, the definition of the cost functional to be minimized using GA; and third, a reduced set of output data (parametrization), used as a strong regularization technique to overcome noise problems.

This data is intended to be used in the most efficient form. For that purpose, it is processed via wavelet decomposition and every component is weighted to select the most efficient ones, from the point of view of maximizing the POD. The POD is approximated from several singular evaluations of the cost functional, and is therefore dependent on the weight filter. This dependency allows to maximize the POD.

Numerical parametric examples shows that the optimal filter proposed in the study allows to find damage of a magnitude several times smaller. A suitable parametrization is essential to give to robustness to the search and the solution, and the proposed methods allow to easily find small damage at noise levels above 50%. The proper choice of measurement points provides a similar improvement in the search sensitivity. Since there do not seem to be simple rules for this choice, a numerical optimization of this choice is proved in this paper to be advantageous.

ACKNOWLEDGEMENTS

This work was supported by the Korea Research Foundation Grant KRF-2005-M01-000-10230-0.

REFERENCES

1. Yang JCS, Tsai T, Pavlin V, Chen J, Tsai WH. Structural damage detection by the system identification technique. *Shock and Vibration* 1985; **55**:57–68.
2. Rizos PF, Aspragathos N, Dimarogonas AD. Identification of crack location and magnitude in a cantilever beam from the vibration modes. *Journal of Sound and Vibration* 1990; **138**:381–388.
3. Ruotolo R, Shifrin EI. Natural frequencies of a beam with arbitrary number of cracks. *Journal of Sound and Vibration* 1999; **223**(3):409–423.
4. Morassi A, Rollo M. Identification of two cracks in a simply supported beam from minimal frequency measurements. *Journal of Sound and Vibration* 2001; **7**:729–739.
5. Boström A, Wirdelius H. Ultrasonic probe modeling and nondestructive crack detection. *Journal of the Acoustical Society of America* 1995; **97**:2836–2848.
6. Suh MW, Shim MB, Kim MY. Crack identification using hybrid neuro-genetic technique. *Journal of Sound and Vibration* 2000; **238**(4):617–635.

7. Mares C, Surace C. An application of genetic algorithms to identify damage in elastic structures. *Journal of Sound and Vibration* 1996; **195**:195–215.
8. Friswell MI, Pennyb JET, Garvey SD. A combined genetic and eigensensitivity algorithm for the location of damage in structures. *Computers and Structures* 1998; **69**:547–556.
9. Chou JH, Ghaboussi J. Genetic algorithms in structural damage detection. *Computers and Structures* 2001; **79**:1335–1353.
10. Krawczuk M. Application of spectral beam finite element with a crack and iterative search technique for damage detection. *Finite Elements in Analysis and Design* 2002; **38**:537–548.
11. Lee SY, Wooh SC. Waveform-based identification of structural damage using the combined fem and microgenetic algorithms. *Journal of Structural Engineering* (ASCE) 2005; **131**(9):1464–1472.
12. Kimoto K, Hirose S. A numerical modelling of contact sh-wave transducers. In *Review of Progress in Quantitative Nondestructive Evaluation*, Thompson DO, Chimenti DE (eds), vol. 20. 2000.
13. Schmerr LW. *Fundamentals of Ultrasonic Nondestructive Evaluation*. Plenum Press: New York, 1998.
14. Zhao J, Gaydecki PA, Burdekin FM. A numerical model of ultrasonic scattering by a defect in an immersion test. *Ultrasonics* 1995; **33**(4):271–276.
15. Rus G, Wooh SC, Gallego R. Analysis and design of wedge transducers using the boundary element method. *Journal of Acoustic Society of America* 2004; **115**:2919–2927.
16. Addison P. The little wave with the big future. *Physics World* 2004; 35–39.
17. Kim IK, Kim YY. Damage size estimation by the continuous wavelet ridge analysis of dispersive bending waves in a beam. *Journal of Sound and Vibration* 2005.
18. Li B, Chen XF, Ma JX, He ZJ. Detection of crack location and size in structures using wavelet finite element methods. *Journal of Sound and Vibration* 2004.
19. Messina A. Detecting damage in beams through digital differentiator filters and continuous wavelet transforms. *Journal of Sound and Vibration* 2004; **272**:385–412.
20. Yang WX, Hull JB, Seymour MD. A contribution to the applicability of complex wavelet analysis of ultrasonic signals. *NDT&E International* 2004; **37**:497–504.
21. Liu PL, Chen CC. Parametric identification of truss structures by using transient response. *Journal of Sound and Vibration* 1996; **191**(2):273–287.
22. Tarantola A, Valette B. Inverse problems = quest for information. *Journal of Geophysics* 1982; **50**:159–170.
23. Au FTK, Cheng YS, Tham LG, Bai ZZ. Structural damage detection based on a micro-genetic algorithm using incomplete and noisy modal test data. *Journal of Sound and Vibration* 2003; **259**(5):1081–1094.
24. Bathe KJ. *The Finite Element Procedures in Engineering Analysis*. Prentice-Hall: Englewood Cliffs, NJ, 1996.
25. Goldberg D. *Genetic Algorithms in Search*, *Optimization and Machine Learning*. Addison-Wesley Publishers: Reading, MA, 1989.
26. Gallego R, Rus G. Identification of cracks and cavities using the topological sensitivity boundary integral equation. *Computational Mechanics* 2004; **33**:154–163.

